

A 3D Self-Consistent Percolative Model for AC-DC Electrical Analysis of Carbon Nanotubes Networks

Simone Colasanti, Vijay Deep Bhatt, Ahmed Abdelhalim, Alaa Abdellah, Paolo Lugli

Institute for Nanoelectronics
 Technical University of Munich
 Munich, Germany
 simone.colasanti@nano.ei.tum.de

Abstract—We present a SPICE-based percolative model for the simulation of randomly aligned networks of carbon nanotubes (CNT). The network generation is based on a stochastic algorithm that randomly generates nanotubes over a substrate according to some statistical distribution inferred from the measurements of real devices. The transport mechanisms are modeled in a multiscale framework. The current of each nanotube is first pre-computed following the theory of one-dimensional channels. The electrical behavior of the entire network is afterwards simulated by coupling a SPICE program with an iterative algorithm that calculates self-consistently the electrostatic potential in each node of the network. Comparisons with AFM images allowed us to validate the model for the network generation, while the results from the simulations have been compared with measurements of devices designed as gas sensors. Particular attention has been focused on the response of the network in the AC regime.

Keywords—CNT Networks, 3D Modeling, Percolation, SPICE Model, CNT Frequency, Complex Impedence.

I. INTRODUCTION

Since their discovery in 1991 [1], carbon nanotubes (CNT) have drawn the attention of many research groups in the scientific community. Despite their amazing electronic and mechanical properties, devices based on single nanotubes have the major drawback of a difficult reproducibility. The lack of a scalable and reliable process for the positioning of an individual nanotube between two electrodes reduces a lot the versatility of such devices. A possible way to overcome this problem is to create an interconnected network of nanotubes, randomly aligned over a substrate, where the individual properties of the single CNT are averaged out by the large number of elements. The big advantage of these films is that they can be easily prepared using cost-efficient deposition methods, such as spray-coating or ink-jet deposition, making them particularly attractive for large-area printed electronic [2]. Among the possible applications, they can be exploited as transparent electrodes, thin films transistors and devices sensible to different environmental changes [3]. The involved deposition processes are usually based on aqueous solutions of unsorted single-wall CNT, which means there is no specific control on the chirality of the nanotubes. Moreover, since the CNTs are randomly deposited over the substrate, the study of the transport through the network is not a trivial task. In this regards, computational models based on the percolation theory

are a powerful tool which can provide important figures of merit in a cost and time efficient way.

In this work we extended the so-called stick-percolation theory into a three-dimensional framework. An unavoidable drawback of two-dimensional models is that the number of junctions between the nanotubes in the network is highly overestimated by the on-plane projections on the substrate. This artifact has a dramatic effect on the reliability of the simulation, especially for dense films. To overcome this limit we developed a model based on a stochastic algorithm that can generate non-rigid solid objects in a three-dimensional space, emulating with high fidelity the fabrication processes involved. Additionally, we introduced a multiscale approach for the study of the conduction through the network. The transport mechanisms in the single nanotubes are modeled according to the theory of one-dimensional ballistic channels based on the computation of the density of states. The behavior of the entire network is then simulated by coupling a SPICE program with an iterative algorithm that calculates self-consistently the electrostatic potential and the current flow in each node of the network. The simulations have been validated by comparison with experimentally measured devices. Our general aim is to provide a tool for the design of these films in a broad range of application. In this work we focused the attention on the frequency response of some films designed to be specifically sensitive to NH_3 gas molecules.

II. NETWORK GENERATION

In this work we referred to our previously developed simulation tool [4]. The first step is the generation of the randomly aligned network, which is done in analogy with the experimental setup used for the fabrication of the devices. The films have been spray-deposited onto an inter-digitated electrode structure (IDES) using an air-atomizing nozzle [5]. Each nanotube is represented as a bendable cylinder with radius and length that are randomly chosen according to some statistical distributions directly inferred by AFM images. While the radius is in a first approximation constant, the length cannot really be predicted a priori. During some process steps, from the agglomerate of CNTs provided by the supplier, to the final sprayed film, the nanotubes can often break. With our setup, the result is usually a narrow lognormal distribution with an average length around 750 nm [6]. The number of nanotubes to be generated is determined by a specific density of $\text{CNT}/\mu\text{m}^2$ which depends on the number of spraying cycles.

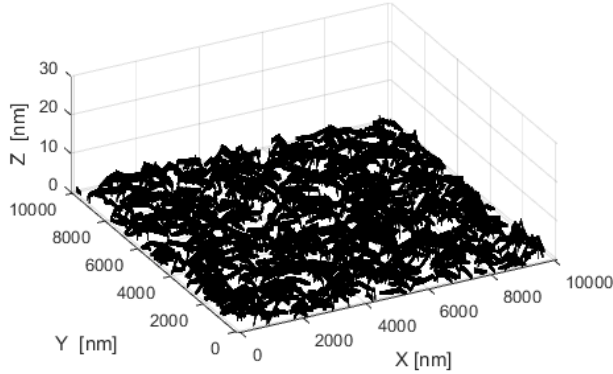


Fig. 1. Three dimensional representation of a generated network with a density of 18 CNT/ μm^2 . The simulation domain is a square region of $10 \times 10 \mu\text{m}^2$.

The CNTs are then placed sequentially, checking each time if there are any intersections between the new nanotube and the already generated network; if an intersection occurs, the new nanotube will be bent with a certain angle which is typically less than 10 degrees. If the angle is greater than the maximum one, the nanotube will slide until it finds a resting point, either directly on the substrate or over another nanotube. The result is a very thin 3D film, as it is shown in Fig. 1. We found a good agreement with the observed samples, both in terms of coverage of the surface and thickness of the film. After this generation step the program will store a first matrix that contains all the coordinates of every node of the network and a second matrix that contains the information on all the connections between the nanotubes. The first matrix contains also the information about the electronic properties of the nanotubes. These are determined by choosing the two indexes of the chiral vector, which are extracted according to a certain solution-dependent probability. In this work we used an aqueous solution of unsorted single-wall CNT (33% metallic, 67% semiconducting) from Carbon Solutions, Inc (CSI).

III. COMPUTATIONAL MODELS

The resulting set of tube segments and tube junctions is then converted into a netlist and the overall electrical behavior is computed by coupling our program with a SPICE software. Prior to that, the IV-characteristic of every nanotube species (i.e. every chirality that has been previously extracted) is pre-computed and stored into a matrix. The value of every single resistance is dynamically calculated within a self-consistent algorithm as explained further below. The expression of the resistance follows the equation:

$$R(V) = R_0(V) \left(1 + \frac{L}{\lambda_{EFF}} \right) \quad (1)$$

where $R_0(V)$ represents the so-called quantum resistance, L is the length of the tube segment and λ_{EFF} is the effective mean free path that contains the effects due to phonon scattering events [7][8]. The quantum resistance is calculated as the ratio between the applied voltage and the current that flows through

the nanotube, which is solved according to the theory of one-dimensional conducting channels [9] and it follows the equation

$$I(V) = \frac{q}{\hbar} \int_{-\infty}^{+\infty} dE D_e(E) \frac{\gamma_1 \gamma_2}{\gamma_1 + \gamma_2} [f_1(E, V) - f_2(E, V)] \quad (2).$$

In (2) q represents the electronic charge, \hbar is the reduced Planck constant, $D_e(E)$ is the density of states per unit of energy, γ_1 and γ_2 are the broadening functions at the contacts. The variable that discriminates the different properties of the CNTs is the DOS, which is computed according to the numerical model developed in [10]. From (2) we can see that the current is a function of the electrostatic potentials imposed at the two contacts of the nanotube (this dependence is implicit in the Fermi functions $f_1(E, V)$ and $f_2(E, V)$ at the two nodes). This requires a self-consistent solution of the two equations, which is usually carried out using an iterative procedure. Starting from an initial guess for the value of the resistance of the nanotubes, the program will calculate the potentials at each node; this information is stored into a matrix and gives us a map of the potential distribution in the network, as it is shown in Fig. 2.

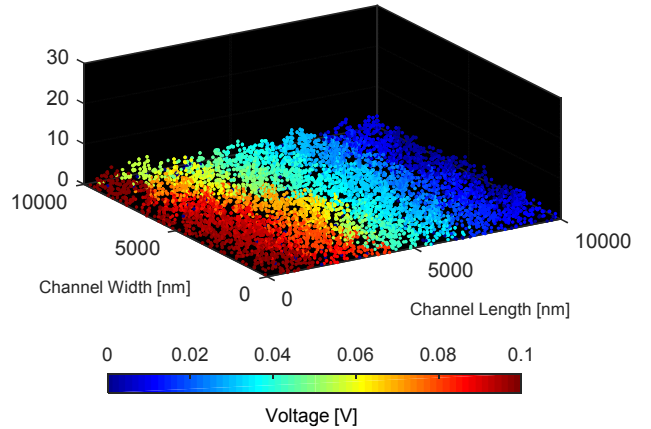


Fig. 2. Three dimensional representation of the potential distribution in the network of Fig. 1.

The value of the resistor will be updated by computing the current with (2) and the process will be iterated until the variations of the potential in each node, between two consecutive iterations, is smaller than a previously set tolerance. Furthermore, in the attempt to simulate the response of the network to an AC stimulus, we replace the simple resistive model for the single nanotube with an equivalent RC circuit, as it is schematically depicted in Fig. 3a. The physical reason for this capacitance is that every nanotube has both the contribution of its own capacitance (i.e. quantum capacitance, which is DOS-dependent) and the coupling capacitance with other nanotubes in the network. The quantum inductance has been neglected on purpose since its effect is visible only for frequency in the GHz range or higher [11]. To complete the picture, we also introduced a parasitic capacitance between the two electrodes, as it is shown in Fig. 3b.

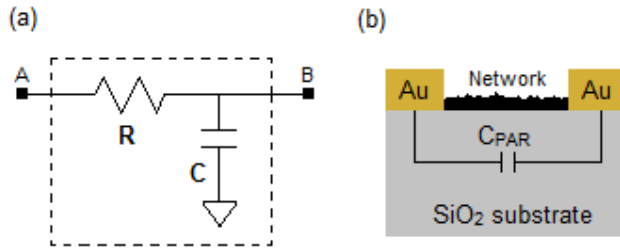


Fig. 3. (a) Equivalent circuit for a single nanotube between node A and node B. (b) Schematic side view of the device. A parasitic capacitance has been imposed between the two gold electrodes.

IV. RESULTS AND DISCUSSION

To validate our model, we performed several simulation comparing our results with the experimental measurements of some films designed as gas sensors. The analysis has been performed by studying the behavior of the complex impedance versus the frequency of the applied AC voltage. We found a good agreement between the measurements and the simulation for several different operating conditions (e.g. temperature and gas concentration) and for different densities of the CNT network. In Fig. 4 we show the real part and the imaginary part of the complex impedance for two network with different densities.

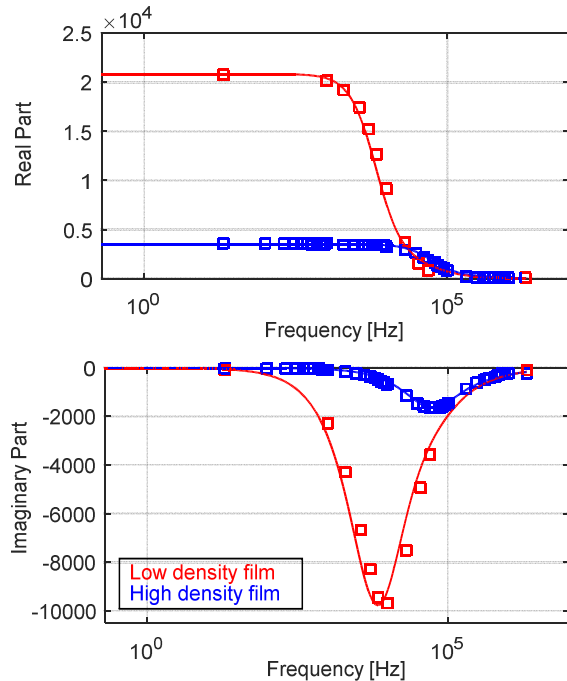


Fig. 4. Real and imaginary part of the complex impedance versus the frequency for different films. The low density film has a density of approximately $12 \text{ CNT}/\mu\text{m}^2$, while the denser one has a density around $20 \text{ CNT}/\mu\text{m}^2$.

The behavior of the entire network is similar to a low-pass filter with a cut-off frequency that depends mainly on the

capacitance of each nanotube. In the model we defined a capacitance per unit of length, with a nominal value of $3 \text{ fF}/\mu\text{m}$ for the high-density network and $12 \text{ fF}/\mu\text{m}$ for the low-density network. These two different values for the capacitance are based on the assumption that when the network is sparser, the coupling capacitance between the nanotubes increases due to the fact that the network is less connected. The results show that denser films have a lower cut-off frequency. By changing the capacitance value of the single nanotubes, we observed a shift in the cut-off frequency, but no effect on the shape of the curve. In Fig. 5 we show how a simple first order model fail to represent properly the behavior of the network. According to our simulation the effect of the parasitic capacitance between the electrodes is not negligible especially for frequencies higher than the cut-off frequency.

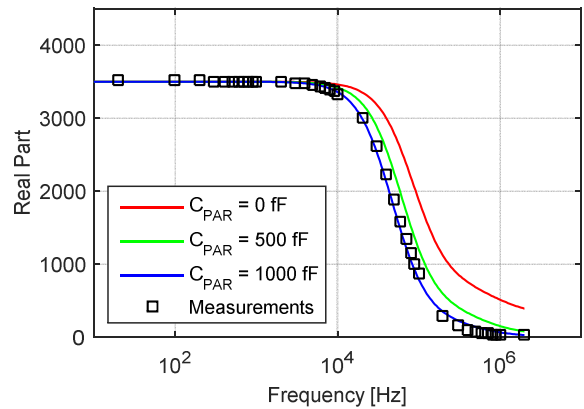


Fig. 5. Real part of the complex impedance versus the frequency for different values of parasitic capacitance.

Furthermore, we analyzed the network under different concentration of NH_3 . It is well known that CNTs in these films exhibit a p-type behavior due to the physisorption of oxygen molecules [12]. Other studies showed how the ammonia has an opposite effect on the electronic structure of the nanotube, inducing an n-doping effect [13]. An increase of the concentration of ammonia makes the network less conductive, since the nanotubes are becoming more intrinsic. This effect tends to saturate for high concentration of gas, since the physisorption of the NH_3 molecules becomes less probable. In our model all these effects are taken into account by shifting the Fermi level of the nanotubes. This will lead to a change in the resistive part of the nanotube, leaving in a first approximation the capacitance unaltered. In Fig. 6 we show the behavior of the real part of the complex impedance for different concentration of ammonia.

The effect of the gas molecules has shown to be also temperature dependent [14]. An increase of the temperature for example, leads to a de-adsorption of the oxygen molecules, which has a different impact on the network depending on the surrounding atmosphere (ambient conditions or controlled atmosphere) [15].

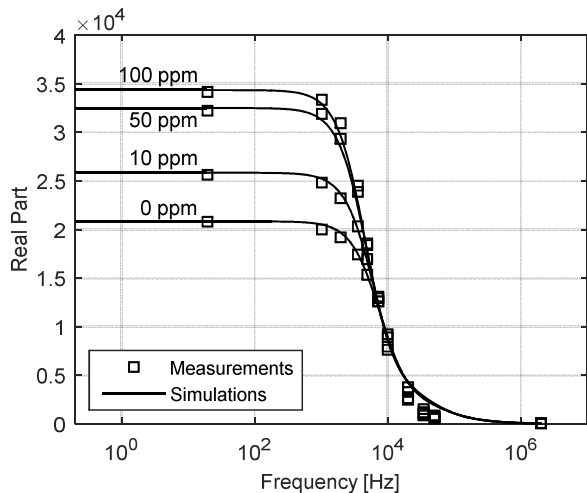


Fig. 6. Real part of the complex impedance versus the frequency for different concentration of NH_3 .

In Fig. 7 we show the results of a network measured in air atmosphere at different temperatures. Also in this case the effect seems to affect predominantly the resistance of the nanotube and not the capacitance which has been kept constant in all the simulations.

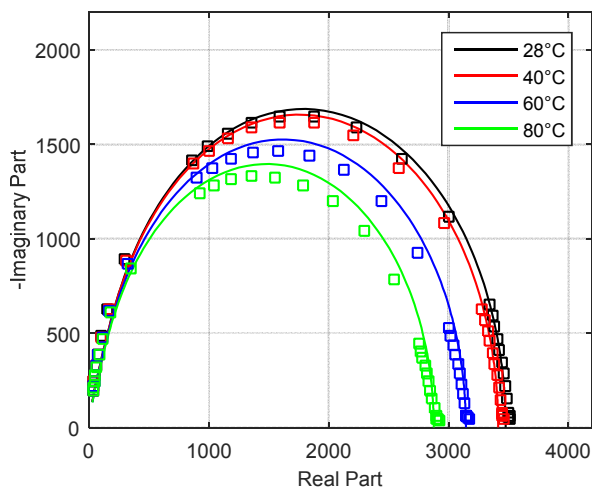


Fig. 7. Nyquist plot of the complex impedance at different temperatures in a frequency range between 20 Hz and 2 MHz.

V. CONCLUSION

In conclusion, we report the modeling of the frequency behavior of various CNT networks under different operating conditions. The good agreement between experimental and computational results allowed us to validate our model. We observed that the frequency behavior is affected by the density of the film, but not on the value of the resistance of the single nanotubes. This can be seen by investigating the behavior of the film under different gas concentrations; the different

amount of molecules alters the resistive part of the nanotube but leaves the reactive part in a first approximation unchanged. Such findings suggest us that the cut-off frequency is related to the number of nanotubes in the network and to the way they arrange on the substrate rather than their resistance value. Finally, we also performed an analysis under different temperatures, observing a similar behavior; the reactive part of the network is indeed nearly unaffected by such variations.

ACKNOWLEDGMENT

This work was supported by the European Commission under grant agreement PITN-GA-2012-317488-CONTEST and the TUM Graduate School.

REFERENCES

- [1] S. Iijima, "Helical microtubules of graphitic carbon," *Nature*, vol. 354, no. 6348, pp. 56–58, 1991.
- [2] A. Abdellah, A. Abdelhalim, M. Horn, G. Scarpa, and P. Lugli, "Scalable spray deposition process for high-performance carbon nanotube gas sensors," *IEEE Trans. Nanotechnol.*, vol. 12, no. 2, pp. 174–181, 2013.
- [3] L. Hu, D. S. Hecht, and G. Grüner, "Carbon nanotube thin films: fabrication, properties, and applications," *Chem. Rev.*, vol. 110, no. 10, pp. 5790–5844, Oct. 2010.
- [4] S. Colasanti, V. D. Bhatt, and P. Lugli, "3D Modeling of CNT Networks for Sensing Applications," in *2014 10th Conference on Ph. D. Research in Microelectronics and Electronics (PRIME)*, 2014, pp. 3–6.
- [5] A. Abdellah, A. Yaqub, and C. Ferrari, "Spray deposition of highly uniform CNT films and their application in gas sensing," *2011 11th IEEE Int. Conf. Nanotechnol.*, pp. 1118–1123, 2011.
- [6] E. Albert, A. Abdellah, G. Scarpa, and P. Lugli, "Electronic transport modeling with HSPICE in random CNT networks," *2012 12th IEEE Int. Conf. Nanotechnol.*, pp. 1–4, Aug. 2012.
- [7] A. Naemi and J. D. Meindl, "Physical Modeling of Temperature Coefficient of Resistance for Single- and Multi-Wall Carbon Nanotube Interconnects," *IEEE Electron Device Lett.*, vol. 28, no. 2, pp. 135–138, Feb. 2007.
- [8] G. Pennington and N. Goldsman, "Low-field semiclassical carrier transport in semiconducting carbon nanotubes," *Phys. Rev. B*, vol. 71, no. 20, p. 205318, May 2005.
- [9] S. Datta, *Quantum Transport: Atom to Transistor*. Cambridge: Cambridge University Press, 2005.
- [10] J. Mintmire and C. White, "Universal Density of States for Carbon Nanotubes," *Phys. Rev. Lett.*, vol. 81, no. 12, pp. 2506–2509, Sep. 1998.
- [11] P. J. Burke, "Luttinger Liquid Theory as a Model of the Gigahertz Electrical Properties of Carbon Nanotubes," *IEEE Trans. Nanotechnol.*, vol. 1, no. 3, pp. 129–145, 2002.
- [12] D. Kang, N. Park, J. Ko, E. Bae, and W. Park, "Oxygen-induced p-type doping of a long individual single-walled carbon nanotube," *Nanotechnology*, vol. 16, no. 8, pp. 1048–1052, Aug. 2005.
- [13] J. Zhao, A. Buldum, J. Han, and J. P. Lu, "Gas molecule adsorption in carbon nanotubes and nanotube bundles," *Nanotechnology*, vol. 13, no. 2, pp. 195–200, Apr. 2002.
- [14] J. L. et al. Barnes, Teresa M.; Blackburn, "Reversibility, Dopant Desorption, and Tunneling in the Temperature-Dependent Conductivity of Type-Separated, Conductive Carbon Nanotube Networks," *ACS Nano*, vol. 2, no. 9, pp. 1968–1976, 2008.
- [15] S. Colasanti, V. Robbiano, F. C. Loghin, V. Deep Bhatt, A. Abdellah, F. Cacialli, and P. Lugli, "Experimental and Computational Study on the Temperature Behavior of CNT Networks," *2015 15th IEEE Int. Conf. Nanotechnol.*, 2015, in press.